Research Square

Preprints are preliminary reports that have not undergone peer review.
They should not be considered conclusive, used to inform clinical practice,
or referenced by the media as validated information.

CDK4/6 inhibition exploits the radiobiology of lutetium-177 therapy to induce replication stress and durable senescence

Edward O'Neill

edward.oneill@nds.ox.ac.uk

University of Oxford

Francesca Amoroso

University of Oxford

Michael Mosley

University of Oxford

Txema Heredia Genestar

Erasmus MC Cancer Institute

Julie Nonnekens

Erasmus MC Cancer Institute

Bart Cornelissen

University Medical Center Groningen

Research Article

Keywords: targeted radionuclide therapy, radioligand therapy, combination therapy, senescence, autophagy, radiobiology

Posted Date: November 4th, 2026

DOI: https://doi.org/10.21203/rs.3.rs-11010972/v1

License: This work is licensed under a Creative Commons Attribution 4.0 International License.
Read Full License

Additional Declarations: No competing interests reported.

Abstract

Background

Lutetium-177 (^{177}Lu)-based radiopharmaceutical therapy delivers prolonged low-dose-rate irradiation, creating a radiobiological context that differs substantially from conventional external beam radiotherapy (EBRT). We hypothesised that this extended radiation exposure generates distinct therapeutic vulnerabilities and senescence states that can be exploited pharmacologically.

Methods

A high-throughput clonogenic screen of 295 small-molecule inhibitors was performed in combination with ^{177}Lu-DOTATATE and compared with equitoxic EBRT. Candidate interactions were validated using multiple CDK4/6 inhibitors across SSTR2- and PSMA-targeted neuroendocrine and prostate cancer models, including xenografts. Cell-cycle regulation, replisome stability, DNA damage, p21 dynamics, senescence and autophagy-associated nuclear processing were interrogated mechanistically.

Results

Drug interactions with ^{177}Lu-DOTATATE differed substantially from those observed with EBRT, identifying CDK4/6 inhibition as a preferential therapeutic vulnerability of prolonged ^{177}Lu exposure. Abemaciclib, palbociclib and ribociclib enhanced clonogenic suppression by ^{177}Lu-DOTATATE, while abemaciclib similarly potentiated ^{177}Lu-PSMA in human prostate cancer models and improved tumour control in vivo. Therapeutic cooperation was not associated with enhanced Rb inhibition or G1 arrest, but with replisome depletion, replication stress, genotoxicity and durable senescence. Distinct senotypes emerged between tumour models: 22Rv1 cells developed a predominantly sustained p21^{high} state associated with persistent growth arrest, whereas CA20948 cells displayed a p21^{low} senotype following an early p21 response, accompanied by increased autophagic and nucleophagic features. Pharmacological inhibition of autophagy differentially altered these senotypes, indicating that divergent p21-processing states can converge on durable senescence following combined CDK4/6 inhibition and ^{177}Lu therapy.

Conclusions

CDK4/6 inhibition exploits a therapeutic vulnerability created by prolonged ^{177}Lu irradiation by promoting replication stress and durable senescence rather than conventional cell-cycle arrest. The emergence of distinct p21^{high} and p21^{low} senotypes identifies senescence heterogeneity as a previously underappreciated determinant of radiopharmaceutical response and provides a mechanistic rationale for combining clinically established CDK4/6 inhibitors with ^{177}Lu-based therapy.

Introduction

Targeted radionuclide therapy (TRT) has emerged as a promising modality for the treatment of cancer, offering a means to selectively deliver cytotoxic radiation to tumour cells while sparing surrounding healthy tissue[1]. Clinical trials with beta-particle emitting radiopharmaceuticals, such as the NETTER-1 and VISION trials have demonstrated the efficacy and safety of TRT with ^{177}Lu-DOTATATE in neuroendocrine tumours targeting somatostatin receptor 2 (sstr2) overexpression, and ^{177}Lu-PSMA in metastatic prostate cancer targeting prostate specific membrane antigen (PSMA) overexpression, respectively. These trials highlight TRT's potential to improve patient outcomes with relatively few and mostly transient side effects [2, 3]. However, many patients do not benefit from the treatment, which remains to be administered with palliative intent, despite significant financial costs. Therefore, improvements are being actively investigated. These include the use of alternative radionuclides emitting e.g. alpha or Auger electron radiation, increasing the amount of radionuclide delivered and/or retained in the target tumour tissue, the employment of TRT in earlier disease stages, or by combining TRT with other drugs [4] [5].

Combinations of drugs and radiation therapy have been studied previously, mainly in the context of External Beam Radiotherapy (EBRT) [6]. However, radiosensitisers targeting growth and repair signalling will likely be affected by differences in discrete high-dose rate fractions of EBRT (1 Gy/min) and the extended low dose-rate TRT (1–2 mGy/h) such as ^{177}Lu-DOTATATE or ^{177}Lu-PSMA. The lower dose rate of ^{177}Lu can be instead viewed as an opportunity to identify novel radiosensitisers tailored to the radiobiology of TRT to target cellular processes particularly over the extended period of radiation exposure. This extended exposure appears critical to cellular responses to ^{177}Lu TRT. Indeed, in our previous investigation, where we imaged the DNA damage repair marker γH2AX *in vivo* for up to 11 days after ^{177}Lu-based TRT, we correlated the efficacy of ^{177} Lu with changes in the DNA damage response between days 5 and 7, and highlighted how senescence appeared to be a key determinant of treatment success [7].

In the current study, a high-throughput clonogenic based drug screen using a 295 compound small molecule inhibitor library was used to identify novel combinations warranting further investigation as radiosensitisers to ^{177}Lu-based TRT. This led to the identification of CDK4/6 inhibitors as an atypical radiosensitiser of TRT resulting in a more durable form of senescence when in combination.

Results

Clonogenic-based drug combination screen with ^{177}Lu-DOTATATE highlights CDK4/6 inhibitors as potent radiosensitisers

To identify drug interactions associated with prolonged ^{177}Lu exposure, we screened 295 small-molecule inhibitors using clonogenic survival after brief exposure to ^{177}Lu-DOTATATE and compared these responses with an equitoxic EBRT condition in sstr2-positive rat low grade neuroendocrine cancer CA20948 cells, a well-studied model of low grade NET. Sequencing of CA20948 cells indicated a mutation profile reflective of G1G2 NETs, with wild type RAS, TP53 and RB1 (See supplemental dataset). Mutations with potentially high impact were found in the histone acetyltransferase Ep300(G715A), the exonuclease exo1(splice donor variant), DNA polymerase kappa POLK (frameshift at 509), and Xrcc6(splice variant), which is involved in non-homologous recombination as a regulatory subunit for the apical DDR kinase DNA-PK.

Cells were exposed briefly to a sublethal amount of ^{177}Lu-DOTATATE (0.32 MBq/mL), or an equitoxic dose of EBRT (2.5 Gy), then highly diluted in media followed by a 14-day exposure to one of the library of drugs, at varying concentrations. As a screening prioritisation metric, we used the combination index (CI) method [8]. We identified several drugs that were synergistic with ^{177}Lu-DOTATATE (CI < 1) (Fig. 1, SI Fig. 1),including compounds that have been previously shown to synergise with ^{177}Lu-DOTATATE, including Poly(ADP-ribose) polymerase (PARP) inhibitors (talazoparib [9], olaparib [10, 11]), and Histone Deacetylase (HDAC) inhibitors (mocetinostat) [12], and mechanistic target of rapamycin (mTOR) inhibitors (sirolimus, temsirolimus, everolimus and deforolimus [13]), thus demonstrating the sensitivity of this screening technique.. Hits further included compounds investigated as radiosensitisers to EBRT, such as the WEE1 inhibitor AZD1775 [14], the Wnt inhibitor XAV-939 [15], chlorpromazine [16], cryptotanshinone [17], farnesyltransferase inhibitor tipifarnib [18], and the BH3 mimetic ABT-737 [19]. Notably, synergistic drugs with TRT do not overlap 1:1 with EBRT treatment. We found a separate set of 17 sensitisers of EBRT that did not sensitise to TRT in this model. Only 40 of the sensitizers of TRT were also sensitizers of EBRT, including a.o. PARP inhibitors (Fig. 1b,d, SI Fig. 1d). Notably, some drugs significantly antagonised the effect of ^{177}Lu-DOTATATE, including Mitogen-Activated Protein Kinase (MEK) inhibitors, and, surprisingly, the antibiotic linezolid (Fig. 1d, SI Fig. 1c).

Hits were validated *in vitro* using increasing activity concentrations of ^{177}Lu-DOTATATE to decrease IC50 values, indicating synergy towards reduction in clonogenicity (Fig. 2). Tipifarnib and abemaciclib demonstrated the clearest ^{177}Lu dose-dependent increase in potency. CDK4/6i (abemaciclib, palbociclib, and ribociclib) and other CDKi (dinaciclib, which inhibits CDK1,2,5,9; and milciclib, a CDK2 inhibitor) all sensitized TRT, indicating a class specific effect (Fig. 2). We focussed on CDK4/6 inhibitors given their widespread clinical use and acceptable safety profile [20]. Abemaciclib proved to be the more efficacious CDK4/6i, causing a marked superadditive effect across the dose-range of ^{177}Lu-DOTATATE (Fig. 2a), with a steady and steep ^{177}Lu dose-dependent decrease in IC50 (Fig. 2f). Abemaciclib was also found to increase in potency with increasing ^{177}Lu-PSMA in PSMA expressing 22Rv1 and LNCaP prostate cancer cells (SI Fig. 2). Others found the radiosensitisation of EBRT by abemaciclib to be dependent on functional p53 [21, 22], which we also saw: synergy of ^{177}Lu-DOTATATE and abemaciclib was not observed in neuroendocrine cancer cell lines with *TP53* mutations (QGP1, BON1, or H727), nor in

LNCaP *TP53* knockout cells treated with ^{177}Lu-PSMA, where it was in LNCaP with p53^{wt}, although abemaciclib monotherapy remained effective in both LNCaP *Tp53*^{wt} and *Tp53*$^{-/-}$ cell lines (SI Fig. 2bc, SI Fig. 3).

In vivo, in a CA20948 xenograft-bearing athymic mouse model, we confirmed that the combination of a sub-therapeutic intravenously administered dose of ^{177}Lu-DOTATATE (7.2 MBq ± 1.2 MBq) based upon previous investigations [7], was synergistic with, starting 24 h after, nine daily administrations of abemaciclib (25 or 50 mg/kg), confirming synergy. This increased therapeutic effect was not accompanied by any signs of gross toxicity, beyond that caused by ^{177}Lu-DOTATATE and anaesthesia for SPECT/CT imaging on day 2 to confirm equivalent ^{177}Lu uptake and retention in the tumour between treatment groups (SI Fig. 2d). Conversely, abemaciclib alone, at those doses, did not inhibit tumour growth (Fig. 2i).

As we performed a naïve drug screen, using a non-enriched drug library, not one category of drugs was presumed. Others have reported DDR-specific libraries, or phosphoproteomics screens [23, 24] to identify potential TRT-drug combination therapies, with partially overlapping hits with our screen (e.g. PARP and DNA-PKcs inhibitors). Moreover, we only looked at drug addition after ^{177}Lu treatment, and in *in vivo* studies only started drug treatment 24 h after the^{177}Lu-compound, when most ^{177}Lu was cleared from most non-targeted tissues, to avoid unwanted synergistic effects in healthy tissues, although we did not investigate these in any further detail here. Other drug scheduling may result in alternative hits, both *in vitro* and *in vivo*, as pre-treatment with drug may affect ^{177}Lu uptake. In our model, abemaciclib treatment did not affect ^{177}Lu retention of tumours, as measured by SPECT imaging 48 h after ^{177}Lu-DOTATATE administration (Fig. 2j). Moreover, we focussed on clonogenic drug screening, as it can prioritise the potential of drugs with both acute and longer-term (e.g. pro-senescence) mechanisms of action. We showed that viability assays would not highlight combinations with CDK4/6i since the acute (e.g. apoptosis) can be overshadowed by the increased metabolic activity of senescent cells (SI Fig. 4). A disadvantage of our screen is that some of the drugs may not hit their target in a rat cell line, used here, and some hits may have been affected by the specific mutational landscape of CA20948. However, we did observe that CDK4/6i synergises with ^{177}Lu-PSMA TRT in 22Rv1 and LNCaP human prostate cancer cells (SI Fig. 2). Finally, a combination index can only provide an approximate indication of synergy (CI < 1) with ionising radiation to prioritise further investigation since the pharmacological mass-action of radiation is not equivalent to that of a conventional drug, with a sigmoidal receptor-ligand dose response.

CDK4 and 6 pair with cyclin D to initiate G1/S transition by phosphorylating Rb. CDK4/6i show significant efficacy in treating hormone receptor-positive, HER2-negative advanced breast cancer, particularly in combination with hormone therapy. This class of drugs has previously been investigated as a radiosensitiser with diverse mechanisms of action including inducing apoptosis [25, 26], reduced colony formation [27], and enhanced DNA damage [28, 29], by modulating autophagy [30], and by decreasing radiation induced vasculogenesis [31, 32]. While never having been prospectively clinically investigated

as a radiosensitiser, it has been shown retrospectively to be well-tolerated with concurrent radiotherapy in breast cancer patients [33]. We therefore investigated some of these mechanisms to provide mechanistic insight into the combination of ^{177}Lu-drugs with CDK4/6i.

TRT + CDK4/6i cooperation does not correlate with Rb hyperphosphorylation or cell cycle

Since CDK4/6i are known to impact the cell cycle by inhibiting the hyperphosphorylation of Rb by the Cyclin D/CDK4 and Cyclin D/CDK6 complexes, we investigated cell cycle effects in 22Rv1 and CA20948 cells as it could account for cell cycle differences in radiation susceptibility, but instead found surprisingly minimal dose-dependent impact of ^{177}Lu-DOTATATE or ^{177}Lu-PSMA on the cell cycle in combination with abemaciclib (SI Fig. 5). We interrogated the relative phosphorylation of Rb further at various timepoints with increasing concentrations of abemaciclib and with and without ^{177}Lu-DOTATATE or ^{177}Lu-PSMA by western blot, yet the enhanced efficacy of the combination of CDK4/6i and ^{177}Lu did not appear to correlate with any further suppression of the hyperphosphorylation of Rb by the Cyclin D/CDK4 and Cyclin D/CDK6 complexes in 22Rv1 (Fig. 3a,b; SI Fig. 6) at the doses used of abemaciclib as a monotherapy or in combination with ^{177}Lu-PSMA, nor any notable changes to the cell cycle, beyond some G2/M arrest by ^{177}Lu-DOTATATE alone (SI Fig. 5).

TRT + CDK4/6i induces replisome instability resulting in genotoxicity and durable senescence

Crozier et al. reported that CDK4/6i induce replication stress by downregulation of replisome components, further exacerbated by addition of chemotherapeutics [34]. We similarly found a depletion of replisome components MCM2, MCM3, and especially PCNA in both cell lines (Fig. 3a; SI Fig. 6). Crozier observed a decrease in the replisome recruiter Cdc6 in their CDK4/6i treated cells over time up to day 7 that was restored upon CDK4/6i washout, potentially driving additional replication stress without other components of the replisome such as PCNA. This *catch-and-release* induction of genotoxicity and replication stress appears also to be occurring in our system, but at sub-therapeutic, low levels of ^{177}Lu-TRT, as Cdc6 is suppressed by abemaciclib at 24 h in 22Rv1 as a monotherapy, but is restored to control levels by day 3, whereas by 24 h Cdc6 is increased in ^{177}Lu-TRT only and in combination treated cells. Cdc6 overexpression has been associated with increased radioresistance [35]. Therefore, this pro-replicative mitogenic drive to release cells into the cell cycle whilst being unprepared, with reduced MCM2/3 and PCNA levels, would be expected to result in replication stress and genotoxicity despite a lack of cell cycle arrest. This partial *catch-and-release* mechanism appears to induce an earlier induction of replication stress in our model compared to that of Crozier et al, indicated by increased levels of γH2AX and p21 at day 3 with sustained p21 levels at day 7 (Fig. 3d). Furthermore, by day 10, we observed a dose-dependent increase in cellular levels of γH2AX in the combination group with the majority of cells with higher amounts of γH2AX (γH2AX^{hi}) in the G2/M phase, with no evidence of further

proliferation given a depletion of EdU+ cells, suggesting that γH2AX in these cells was not caused by current replication stress, but potentially G2 cell-cycle exit from prior replication stress to G2 cell cycle arrest (Fig. 3e) [36]. After ^{177}Lu-PSMA monotherapy, those 22Rv1 cells with elevated γH2AX were found in the EdU + S-phase. This was not significantly different to controls, suggesting a potential baseline susceptibility to replication stress. There were higher levels of γH2AX in 22Rv1 cells exposed to the combination versus ^{177}Lu-PSMA alone at day 3 vs day 1 (Fig. 3; SI Fig. 7), suggesting replication stress. However, this enhancement of γH2AX was lost from day 7, possibly indicating a period of frustrate-release-crash from day 3 [37]. Yet, formation of mono-ubiquitinated γH2AX from day 7, visible in western blots, is also indicative of replication stress [38]. This day 3 crash does not appear to be predominantly due to apoptosis as there were significant levels of pro-Cas 3 after 1000 nM of abemaciclib, but not significantly elevated levels of cleaved Cas3 or cleaved PARP1 (Fig. 3c, SI Fig. 8). We have previously observed that sustained elevated levels of γH2AX post ^{177}Lu exposure were associated with senescence [39]. We found here that CDK4/6i increased senescence associated with sustained high levels of p21 in 22Rv1 cells (Fig. 3f). This appeared to cooperate with increasing activities of ^{177}Lu-PSMA particularly at lower concentrations of abemaciclib (Fig. 3g). The ratio of senescent to apoptotic cells at day 10 was much greater with the addition of abemaciclib, whereas this ratio was static with increasing activities of ^{177}Lu-PSMA monotherapy (Fig. 3h). The interaction between CDK4/6i and ^{177}Lu-PSMA appears to be complex across the concentrations of both CDK4/6i and ^{177}Lu-PSMA, indicating that although there is overall a much greater induction of senescence, there could also be several alternate cell death pathways being activated. This bimodal mechanism of action at low versus higher doses of CDK4/6i has previously been observed by others [40, 41]. We observed key differences between EBRT and ^{177}Lu-PSMA in the induction of senescence at the lower dose of 50 nM of abemaciclib, but this enhancement appeared saturated by the effect of abemaciclib alone when using 200 nM (Fig. 3i). However, despite the same apparent incidence of elevated SA-β-Gal at 200 nM, there was much greater induction of genotoxicity, in particular micronuclei formation (Fig. 3j). This increased level of genotoxicity in the combination with ^{177}Lu-PSMA and abemaciclib manifested in increasing the incidence of permanent senescence, but not by either monotherapy, the latter contrarily resulting in colony regrowth at longer incubation times (Fig. 3k). The same was true for CA20948 cells exposed to ^{177}Lu-DOTATATE and abemaciclib compared to abemaciclib alone (SI Fig. 9). Further interrogation of 22Rv1 colonies that did not regrow in the combination condition appear to be associated with elevated and retained expression of p21 (Fig. 3l). While at day 3, this elevated p21 expression occurs almost entirely in G2, by day 10 elevated p21 is seen in both G1 and G2/S phases of the cell cycle (SI Fig. 10) which aligns well with previous accounts of chemotherapy-induced p21 dynamics [42].

TRT + CDK4/6i co-operates to induce senescence with either a p21 or p21 senotype

Replication stress was also evident in CA20948 cells, TP53^{wt} with mismatched depletion of PCNA and MCM3, with concomitant increased expression of Cdc6 (SI Fig. 6a). However, after an initial burst of

γH2AX and p21 at day 1, there was a loss of γH2AX and p21 protein content in CA20948 cells after combination therapy versus ^{177}Lu-DOTATATE alone at day 3, unlike in 22Rv1 cells (Fig. 4a,b). Further interrogation of γH2AX foci up to day 10 did not reveal any clear differences between ^{177}Lu-DOTATATE alone compared to combination with abemaciclib in cells in G1 or G2/S/M gates (Fig. 4c). Furthermore, there appeared to be a saturation of γH2AX foci beyond 0.32 MBq/mL, which coincidently corresponded to the 0.7 survival fraction of our initial clonogenic screen with ^{177}Lu-DOTATATE. This was not attributed to detection limits as foci in each cell were acquired using a complete Z-stack using a spinning disk confocal microscope (Andor Dragonfly, Oxford Instruments, UK). Instead, we hypothesized that this clearance of p21 and γH2AX-associated damaged histones may be due to increased activation of autophagy through fluctuations in LCBI/II levels (Fig. 4a). Reduction in histone content (including H2AX) has been similarly found in replicative senescence, where these proteins are degraded through autophagy [43]. Indeed, CDK4/6i are known to affect autophagy through the suppression of autophagic cycling, resulting in an atypical type 2 form of autophagic cell death previously encountered in p53^{wt} cell lines [44]. We similarly observed these vacuoles in p53^{wt} CA20948 cells, and we also observed a heterogenous response with many p21^{hi} cells with elevated levels of LCBI/II (Fig. 4d). This suggested a potential macroautophagic response to clear excess p21 as a potential anti-senescence resistance mechanism following CDK4/6i treatment in combination with ^{177}Lu-TRT. To interrogate this autophagic resistance mechanism, we employed the autophagy inhibitor hydroxychloroquine (HCQ), which acts through alkalinisation of intracellular organelles using both CA20948 and 22Rv1 cells. Although HCQ acts on multiple mechanisms, we found that HCQ was only co-operative with ^{177}Lu TRT in CA20948, but not 22Rv1 cells (Fig. 4e). CDK4/6i have been shown to be synergistic with HCQ [40], and clinically well tolerated [45]. We confirmed that HCQ synergistically cooperated with abemaciclib in our model (SI Fig. 11), but interestingly this synergy decreased with the addition of ^{177}Lu-DOTATATE (MuSyC log alpha 3.1 (95%CI [6.9, 2.7]) down to 1.4 (95%CI [2.3, 0.3]) (SI Fig. 11), suggesting that the inhibition of autophagy interfered with a therapeutic autophagic mechanism of action of CDK4/6i with TRT. Furthermore, the addition of HCQ to abemaciclib in 22Rv1 cells appears to be radioprotective, reducing the incidence of senescence particularly significant at higher concentrations of ^{177}Lu-PSMA (SI Fig. 12), while apoptosis remains largely unaffected, suggesting that the therapeutic autophagic mechanism of action of CDK4/6i with TRT in 22Rv1 is pro-senescent. We found that the proportion of p21^{hi} cells were unaffected by the addition of HCQ to our CDK4/6i+^{177}Lu combination, and only significantly reduced the senescent p21^{high} cells at high activity concentrations of ^{177}Lu-PSMA (SI Fig. 13,14). While high levels of p21 are traditionally associated with senescence, an alternative pathway to senescence can occur with low levels of p21 [42]. HCQ appears to predominantly affect the population of abemaciclib-induced senescent cells with high levels of SA-β-Gal that are p21^{low}, with and without radiation (SI Fig. 13,14). So, while CDK4/6i+^{177}Lu-induced senescence appears to be dominated by sustained p21^{high} levels, the p21^{low} senotype appear to be induced through autophagy. Further analysis of p21 levels within the clusters of cells that were unsuccessful at forming colonies, the proportion between p21^{high} and p21^{low} colonies greatly differs between CA20948 and 22Rv1 cells (Fig. 3l). This aligns with CA20948 being

more sensitive to HCQ addition when combined with ^{177}Lu-TRT. Abemaciclib therefore appears capable of inducing both p21^{high} and p21^{low} senotypes that are further enhanced by the addition of ^{177}Lu.

TRT + CDK4/6i overcomes nucleophagic radioresistance clearance of damaged chromatin in p21 senotype

We investigated the radiobiology of this p21^{low} senotype further in CA20948 cells to understand more how autophagy could contribute to a potential radioresistance mechanism against 177Lu-TRT. Interestingly, CA20948 cells did not observe the same pattern of overall increased micronuclei formation as in 22Rv1 (Fig. 3j), following exposure to abemaciclib alone and in combination with TRT (Fig. 4f). We also did not observe any clear sustained levels of p21 (Fig. 4a,b). This apparent lack of increased genotoxicity or p21 could not account for the observed increase in senescence (Fig. 4g), and permanent senescence (SI Fig. 9). We did however observe an increase in Hoechst staining within the cytoplasm, indicative of cytoplasmic chromatin fragments (CCF) (Fig. 4h). These are a known alternative inducer of senescence which are normally cleared by autophagy unless autophagic lysosomes are inhibited [43, 46]. Recently p53 activity has been found to supress CCF [47], which could account for the lack of CCF in ^{177}Lu-DOTATATE monotherapy treated samples compared to those treated with CDK4/6i with senescence associated SA-β-Gal activity (SI Fig. 15). Nucleophagy is the selective degradation of damaged nuclear components through the interaction of LC3 and the nuclear lamin B1 protein and the disruption of this pathway reduces the induction of senescence [48]. We found widespread accumulation of LC3 in the nucleus of cells treated with ^{177}Lu-TRT and CDK4/6i, and in combination. LC3 appears to accumulate mainly in the nucleolus (Fig. 4h). LC3 is known to transiently survey the nucleus under basal conditions [49], but in response to genotoxic stress LC3 can accumulate in the nucleolus. [50] The nucleolus is also known to absorb and accumulate excess p21 [50], and the LC3 nucleolar mediated clearance mechanism has been shown to decrease p21 and decrease senescence and SA-β-gal [51]. However, p21 itself can negatively regulate autophagy through Akt and ROS upregulation [52], highlighting a potential opportunity for CDK4/6i to tip the balance between autophagy and pro-senescence nuclear localised p21. The induction of autophagy in response to elevated p21 could be observed between clusters of CA20948 cells at earlier time points, highlighting the heterogenous bifurcation of p21^{high} and p21^{low} response to ^{177}Lu-TRT (Fig. 4d). We found that CDK4/6i resulted in increased stressed nucleoli with LC3 present, but moreover we found increased levels of p21 outside of these stressed nucleoli indicative of saturated nucleoli incapable of absorbing any more p21 (Fig. 4i). These stressed nucleoli were prevalent in response to both ^{177}Lu and CDK4/6i and were exacerbated in combination, with increasing doses of abemaciclib at day 7, and were retained at day 10 (Fig. 4j). Therefore, since there appears to be an active nucleophagic clearance mechanism, the requirement of high levels of p21 do not appear to be necessary to induce senescence, but rather just enough p21 beyond the capacity to sequester and absorb p21 within these stressed nucleoli. This lack of capacity to absorb p21 in the nucleolus could also be indicative of excessive high-order protein assemblies recently observed in cells undergoing senescence [53]. In addition, in cells exposed to ^{177}Lu-drug followed by

abemaciclib, we observed nucleolar and cytoplasmic Annexin V staining (SI Fig. 16). First reported in 1992, this pattern of Annexin V staining has been previously indicative of nucleolar stress [54]. The dysfunctional release of CCF into the cytoplasm also appears to coincide with p21 and p53 (SI Fig. 17). It is hypothesised that this represents a failed attempt to clear the nucleus of p21 through a disrupted nucleophagic process and how CDK4/6i affects this process warrants further investigation. Although the presence of CCF is traditionally associated with a potentially anti-inflammatory senescence associated secretory phenotype (SASP), we did not find any evidence of the usual markers of SASP (SI Fig. 18). This may be attributed to CDK4/6i induced senotypes being known to produce a different secretory phenotype through p53 and p21 mediated p21/p53 associated secretory phenotype (PASP) [55].

Discussion

We have demonstrated the potential for clonogenic-based drug screens to discover promising combinations to improve the efficacy of TRT. Due to the capacity for clonogenic based screen to highlight drug combinations that induce both senescence and traditional cell death pathways we have uncovered for the first time the cooperative synergy of CDK4/6i and ^{177}Lu based TRT alongside other cytostatic inhibitors that may have been overlooked with typical metabolic-based assays. We have demonstrated that CDK4/6i can enhance subtherapeutic levels of ^{177}Lu in preclinical models of neuroendocrine tumours and prostate cancer highlighting their potential to more effectively treat regions of tumours with low uptake and induce durable permanent senescence.

We investigated the radiobiology of this drug combination further and our results are consistent with earlier results on TRT and CDK4/6i biology, in that the combination of ^{177}Lu-PSMA and ^{177}Lu-DOTATATE with abemaciclib results in p21 cascade and replication stress, causing permanent senescence through p53-p21 mediated genotoxicity and replication stress. Importantly, we have demonstrated that CDK4/6i appear capable of inducing senescence in both p21^{high} and p21^{low} senotypes highlighting its robustness being capable of inducing multiple cellular fates in cell lines with differing TP53 status.

In addition, the potential loss of histones in the formation of a p21^{low} senotype through the combination of CDK4/6i and ^{177}Lu warrants further investigation as the loss of histones has been implicated as a potentially deep senescence senotype associated with reduced malignancy [43].

We have also uncovered to our knowledge for the first time the involvement of nucleolar nucleophagic clearance as a potential resistance mechanism towards TRT and highlighted the need to consider alternative markers of genotoxicity such as cytoplasmic chromatin fragments (CCFs). The potential impact of nucleoli to affect radiation sensitivity warrants further investigation since prominent nucleoli are a classic histopathological feature of aggressive NETs [56], and higher Gleason grade prostate cancer [57]. Just before submission of this manuscript, CDK4/6i was found to reduce the expression of CCFs causing a reduction in SASP via lower cGAS-STING activation in fibroblasts following a single 20 Gy fraction of EBRT [58]. We did not observe any CCFs with our cells treated with ^{177}Lu which may be

due to the lower dose and dose rate anticipated with ^{177}Lu-DOTATATE, and could account for one of the potential reasons why we in saw key differences in cooperativity between EBRT and ^{177}Lu-DOTATATE with CDK4/6i. Also we observed many cells with CCFs treated with CDK4/6i as a monotherapy and combination with ^{177}Lu and this could be due to our use of sub-therapeutic nM concentrations compared to the 2 μM concentrations used in that study.

Abemaciclib has been found to be well tolerated in the treatment of prostate cancer [59], but was not found to be sufficiently efficacious in combination with abiraterone in castration resistant prostate cancer [60]. Ribociclib was found to have efficacy with acceptable toxicity in combination with docetaxel [61]. In addition, palbociclib did not demonstrate any efficacy as a monotherapy in a pre-treated cohort of advanced G1/2 pNETs [62]. A lack of durable permanent senescence in prostate cancer with CDK4/6i has been implicated as a potential cause of clinical resistance from intermittent drug cycles in a recent prostate cancer PDX study [61], and analysis of the LEEP trial evaluating ribociclib in hormone naive high risk prostate cancer in a window trial prior to prostatectomy implicated regions of high proliferation as a cause of resistance to ribociclib [63]. However, we have demonstrated that the senescence induced in combination with ^{177}Lu and abemaciclib are permanent compared to abemaciclib alone and appear to operate by a different senotype without the potentially deleterious effect of SASP associated with prostate therapy-induced treatment resistance [63], recently as well abemaciclib treatment was found to reduce the NF-κB-associated SASP (NASP) [64]. In addition, the p21^{low} senotype has recently been observed in treated fibroblasts with reduced SASP compared with p21^{high} senotypes within a heterogenous cellular population [65].

This co-operative interaction between clinically approved ^{177}Lu-TRT and CDK4/6i occurred at typically subtherapeutic doses, providing a strong rationale for prospective clinical evaluation of this combination

Methods

Full methodological details are laid out in the supplementary information.

PSMA-positive human Prostate Carcinoma 22Rv1 cells (ATCC) or sstr2-postive low-grade rat neuroendocrine cancer CA20948 cells were culture as previously described. Cells were authenticated by the provider. 22Rv1 cells were authenticated by STR profiling. Cells were regularly assessed for the absence of mycoplasma and cultured no longer that twenty passages following resuscitation from liquid nitrogen storage.

^{177}Lu-DOTATATE, ^{177}Lu-PSMA (DOTA-PSMA-I&T) was synthesised as previously described [7, 66], with precursors obtained from ABX, and non-carrier-added ^{177}Lu purchased from ITM, to an apparent molar activity of 50 MBq/nmol for ^{177}Lu-DOTATATE and 40 MBq/nmol for ^{177}Lu-PSMA.

Cells were harvested using Accutase (BioLegend UK), and exposed to ^{177}Lu-PSMA (for 22Rv1 cells) or ^{177}Lu-DOTATATE (for CA20948 cells), at varying activity concentrations for 2 h (or an equitoxic amount

of external beam radiation, delivered by ^{137}Cs irradiation, 1 Gy/min), in aliquots of 1 million cells/mL, diluted in media and grown in cell growth medium containing one of a panel of drugs at varying concentrations (Selleckchem, L1100). Clonogenic survival was assessed after 10–14 days after staining of colonies using crystal violet. Alternatively, viability was measured after 7 days (CellTiter-Glo® 2.0 Cell Viability Assay, Promega).

Alternatively, after brief incubation wtih radiopharmaceutical, followed by one drug, cells were fixed at 1, 2, 3, 5, 7, or 10 days, and stained with DAPI and for various markers for confocal microscopy, or high throughput fluorescence microscopy using Andor Dragonfly equipment, or lysed without fixation, and process for western blot staining for a range of cell signalling, cell cycle, cell stress response, and replisome markers. Antibody details are laid out in full in the supplementary information.

In vivo studies: To evaluate efficacy of the combination of one combination treatment, CA20948 xenograft tumours were established subcutaneously in athymic BALB/cOlaHsd-Foxn1nu mice (Envigo). After 14 days when tumours reached approx. 200 mm^3, animals were administered a sub-therapeutic amount of ^{177}Lu-DOTATATE (7.2 ± 1.2 MBq). From the following day, mice were administered CDK4/6 inhibitor abemaciclib (25 or 50 mg/kg) daily, for 10 days and tumours were measured by calliper. Animal studies were performed under a licence as per the animals (scientific procedures) act, with local ethical committee approval.

Declarations

Acknowledgements.

Technical assistance: Rhodri Wilson (Dept Oncology, Oxford University). LNCaP p53 KO (Peter Nelson, Fred Hutchinson Cancer Center). BON1 (Simona Glasberg, Hadassah Medical Center), BON1^{sstr2}, QGP1^{sstr2} (Carsten Grötzinger, Charité University Medicine Berlin)

Funding
This work was supported by Cancer Research UK (CRUK) through the Gray Institute for Radiation Oncology and Biology, the Medical Research Council (MRC), Prostate Cancer UK (PCUK; grant TLD-CAF22-003), and the John Fell Fund. The funding bodies had no role in the design of the study; collection, analysis, or interpretation of the data; or writing of the manuscript.

Ethics approval and consent to participate

All animal experiments were conducted under licence PA1B5C52F and in accordance with applicable local ethical and regulatory requirements. Consent for publication: Not applicable.

Author Contributions.

EON: Conceptualization, Methodology, Investigation, Formal analysis, Visualization, Project administration, Funding acquisition, Writing – original draft, Writing – review & editing. FA: Investigation, Formal analysis, Writing – review & editing. MM: Investigation. THG: Formal analysis. JN: Resources, Writing – review & editing. BC: Conceptualization, Formal analysis, Funding acquisition, Supervision, Writing – review & editing.

Competing Interests statement.

The authors declare no competing interests. BC holds patents on several radiopharmaceuticals, unrelated to this work. BC and JN acted as paid consultant for companies involved in radiopharmaceuticals development, unrelated to this work. BC and JN have received research funding from companies involved in radiopharmaceutical development, unrelated to this work.

Data Availability Statement

All data generated or analysed during this study are included in this published article and its supplementary information files. The supplementary information includes Supplementary Figures 1–18, Supplementary Dataset 1 (clonogenic drug screen CI values), Supplementary Dataset 2 (sequencing results), and supplementary methods, including antibody details.

References

1. Sgouros G, Bodei L, McDevitt MR, Nedrow JR. Radiopharmaceutical therapy in cancer: clinical advances and challenges. Nat Rev Drug Discov. 2020;19:589–608.
2. Strosberg J, El-Haddad G, Wolin E, Hendifar A, Yao J, Chasen B, et al. Phase 3 trial of 177Lu-Dotatate for midgut neuroendocrine tumors. N Engl J Med. 2017;376:125–35.
3. Sartor O, de Bono J, Chi KN, Fizazi K, Herrmann K, Rahbar K, et al. Lutetium-177-PSMA-617 for Metastatic Castration-Resistant Prostate Cancer. N Engl J Med. 2021;385:1091–103.
4. Terry SYA, Nonnekens J, Aerts A, Baatout S, de Jong M, Cornelissen B, et al. Call to arms: need for radiobiology in molecular radionuclide therapy. Eur J Nucl Med Mol Imaging. 2019;46:1588–90.
5. Chan TG, O'Neill E, Habjan C, Cornelissen B. Combination Strategies to Improve Targeted Radionuclide Therapy. J Nucl Med. 2020;61:1544–52.
6. Sharma RA, Plummer R, Stock JK, Greenhalgh TA, Ataman O, Kelly S, et al. Clinical development of new drug-radiotherapy combinations. Nat Rev Clin Oncol. 2016;13:627–42.
7. O'Neill E, Kersemans V, Allen PD, Terry SYA, Torres JB, Mosley M, et al. Imaging DNA Damage Repair In Vivo After 177Lu-DOTATATE Therapy. J Nucl Med. 2020;61:743–50.
8. Chou T-C. Drug combination studies and their synergy quantification using the Chou-Talalay method. Cancer Res. 2010;70:440–6.
9. Cullinane C, Waldeck K, Kirby L, Rogers BE, Eu P, Tothill RW, Enhancing the anti-tumour activity of 177Lu-DOTA-octreotate radionuclide therapy in somatostatin receptor-2 expressing tumour models

by targeting PARP. Sci Rep. Springer Science and Business, Media LLC et al. 2020;10:10196.

10. Nonnekens J, van Kranenburg M, Beerens CEMT, Suker M, Doukas M, van Eijck CHJ, et al. Potentiation of Peptide Receptor Radionuclide Therapy by the PARP Inhibitor Olaparib. Theranostics Ivyspring Int Publisher. 2016;6:1821–32.
11. Ruigrok EAM, Verkaik NS, de Blois E, de Ridder C, Stuurman D, Roobol SJ, et al. Preclinical Assessment of the Combination of PSMA-Targeting Radionuclide Therapy with PARP Inhibitors for Prostate Cancer Treatment. Int J Mol Sci [Internet]. 2022;23. https://doi.org/10.3390/ijms23148037.
12. Qin Y, Imobersteg S, Frank S, Blanc A, Chiorazzo T, Berger P, et al. Signaling Network Response to alpha-Particle-Targeted Therapy with the (225)Ac-Labeled Minigastrin Analog (225)Ac-PP-F11N Reveals the Radiosensitizing Potential of Histone Deacetylase Inhibitors. J Nucl Med. 2023;64:873–9.
13. Pool SE, Bison S, Koelewijn SJ, van der Graaf LM, Melis M, Krenning EP, et al. mTOR inhibitor RAD001 promotes metastasis in a rat model of pancreatic neuroendocrine cancer. Cancer Res Am Association Cancer Res (AACR). 2013;73:12–8.
14. Cuneo KC, Morgan MA, Davis MA, Parcels LA, Parcels J, Karnak D, et al. Wee1 Kinase Inhibitor AZD1775 Radiosensitizes Hepatocellular Carcinoma Regardless of TP53 Mutational Status Through Induction of Replication Stress. Int J Radiat Oncol Biol Phys. 2016;95:782–90.
15. Zhang J, Si J, Gan L, Guo M, Yan J, Chen Y, et al. Inhibition of Wnt signalling pathway by XAV939 enhances radiosensitivity in human cervical cancer HeLa cells. Artif Cells Nanomed Biotechnol. 2020;48:479–87.
16. Shenoy MA, Biaglow JE, Varnes ME, Daniel JW. A biochemical basis for the radiosensitizing and cytotoxic effects of chlorpromazine hydrochloride in vitro and in vivo. Int J Radiat Oncol Biol Phys. 1982;8:725–8.
17. Li X, Li W, Yang P, Zhou H, Zhang W, Ma L. Anticancer effects of Cryptotanshinone against lung cancer cells through ferroptosis. Arab J Chem. 2021;14:103177.
18. Haas-Kogan DA, Banerjee A, Poussaint TY, Kocak M, Prados MD, Geyer JR, et al. Phase II trial of tipifarnib and radiation in children with newly diagnosed diffuse intrinsic pontine gliomas. Neuro Oncol. 2011;13:298–306.
19. Li J-Y, Li Y-Y, Jin W, Yang Q, Shao Z-M, Tian X-S. ABT-737 reverses the acquired radioresistance of breast cancer cells by targeting Bcl-2 and Bcl-xL. J Exp Clin Cancer Res. 2012;31:102.
20. Wang X, Zhao S, Xin Q, Zhang Y, Wang K, Li M. Recent progress of CDK4/6 inhibitors' current practice in breast cancer. Cancer Gene Ther Springer Sci Bus Media LLC. 2024;31:1283–91.
21. Naz S, Leiker AJ, Choudhuri R, Preston O, Sowers AL, Gohain S, et al. Pharmacological Inhibition of HSP90 Radiosensitizes Head and Neck Squamous Cell Carcinoma Xenograft by Inhibition of DNA Damage Repair, Nucleotide Metabolism, and Radiation-Induced Tumor Vasculogenesis. Int J Radiat Oncol Biol Phys. 2021;110:1295–305.
22. Fernandez-Aroca DM, Roche O, Sabater S, Pascual-Serra R, Ortega-Muelas M, Sanchez Perez I, et al. P53 pathway is a major determinant in the radiosensitizing effect of Palbociclib: Implication in

cancer therapy. Cancer Lett. 2019;451:23–33.

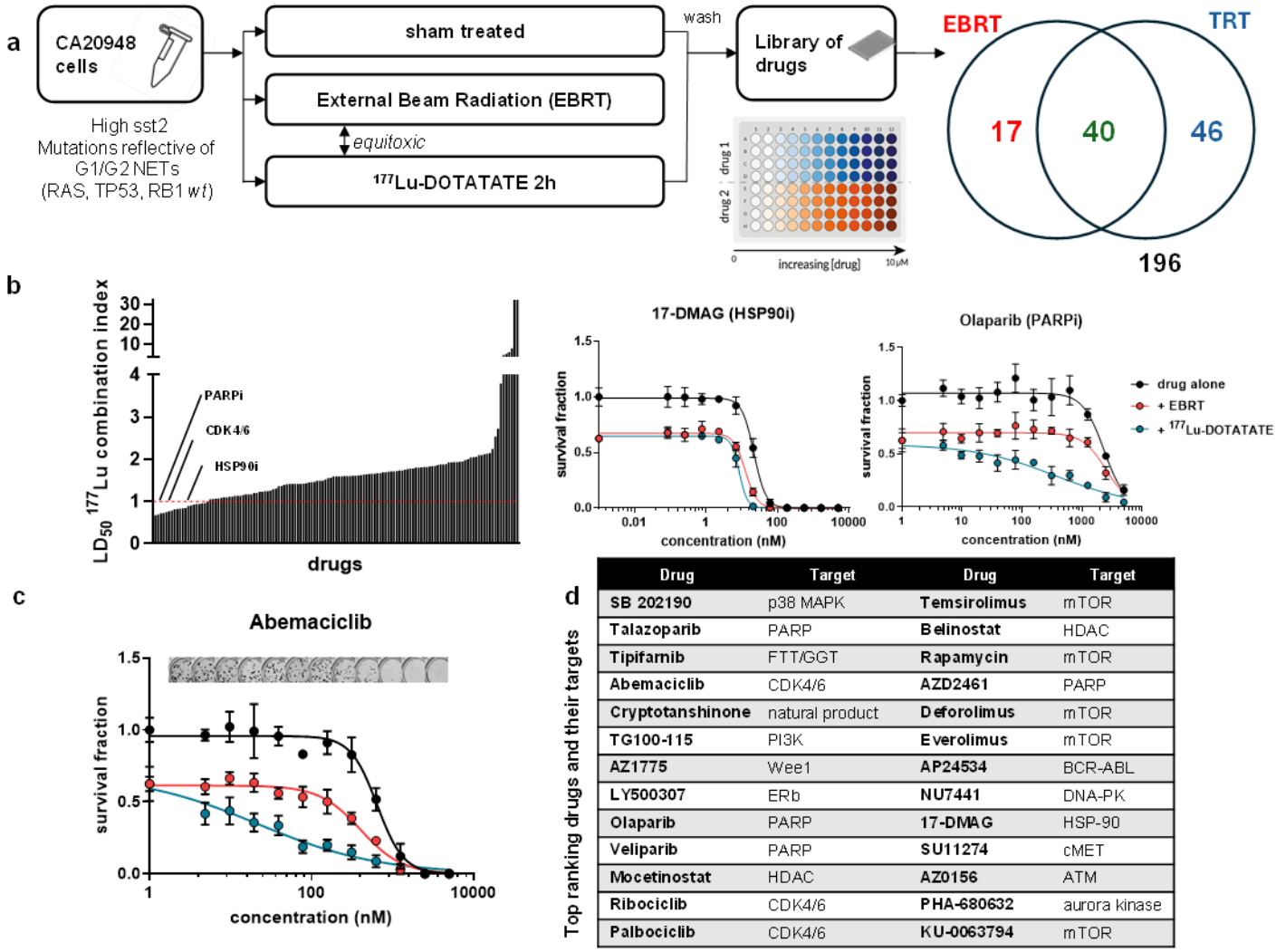
23. Grzmil M, Boersema P, Sharma A, Blanc A, Imobersteg S, Pruschy M, et al. Comparative analysis of cancer cell responses to targeted radionuclide therapy (TRT) and external beam radiotherapy (EBRT). J Hematol Oncol. 2022;15:123.
24. Reuvers TGA, Heredia-Genestar JM, Garrido-Hernandez G, Brandt RMC, Tamborino G, Nonnekens J. Preclinical comparison of radiobiological and radiosensitizing effects in peptide receptor radionuclide therapy and external beam radiotherapy. EANM Innov Elsevier BV. 2026;3:100274.
25. Hagen KR, Zeng X, Lee M-Y, Tucker Kahn S, Harrison Pitner MK, Zaky SS, et al. Silencing CDK4 radiosensitizes breast cancer cells by promoting apoptosis. Cell Div. 2013;8:10.
26. Whittaker S, Madani D, Joshi S, Chung SA, Johns T, Day B, et al. Combination of palbociclib and radiotherapy for glioblastoma. Cell Death Discov. 2017;3:17033.
27. Whiteway SL, Harris PS, Venkataraman S, Alimova I, Birks DK, Donson AM, et al. Inhibition of cyclin-dependent kinase 6 suppresses cell proliferation and enhances radiation sensitivity in medulloblastoma cells. J Neurooncol. 2013;111:113–21.
28. Hashizume R, Zhang A, Mueller S, Prados MD, Lulla RR, Goldman S, et al. Inhibition of DNA damage repair by the CDK4/6 inhibitor palbociclib delays irradiated intracranial atypical teratoid rhabdoid tumor and glioblastoma xenograft regrowth. Neuro Oncol. 2016;18:1519–28.
29. Huang CY, Hsieh FS, Wang CY, Chen LJ, Chang SS, Tsai MH, et al. Palbociclib enhances radiosensitivity of hepatocellular carcinoma and cholangiocarcinoma via inhibiting ataxia telangiectasia-mutated kinase-mediated DNA damage response. Eur J Cancer. 2018;102:10–22.
30. Nardone V, Barbarino M, Angrisani A, Correale P, Pastina P, Cappabianca S, et al. CDK4, CDK6/cyclin-D1 Complex Inhibition and Radiotherapy for Cancer Control: A Role for Autophagy. Int J Mol Sci [Internet] mdpi com. 2021;22. https://doi.org/10.3390/ijms22168391.
31. Naz S, Cook JA, Mitchell JB, Abemaciclib. A multi-functional radiation modifier. Oncotarget ncbi nlm nih gov. 2019;10:1230–2.
32. Naz S, Sowers A, Choudhuri R, Wissler M, Gamson J, Mathias A, et al. Abemaciclib, a Selective CDK4/6 Inhibitor, Enhances the Radiosensitivity of Non-Small Cell Lung Cancer In Vitro and In Vivo. Clin Cancer Res. 2018;24:3994–4005.
33. Kubeczko M, Gabrys D, Gawkowska M, Polakiewicz-Gilowska A, Cortez AJ, Krzywon A, et al. Safety and Feasibility of Radiation Therapy Combined with CDK 4/6 Inhibitors in the Management of Advanced Breast Cancer. Cancers (Basel) [Internet]. 2023;15. https://doi.org/10.3390/cancers15030690.
34. Crozier L, Foy R, Mouery BL, Whitaker RH, Corno A, Spanos C, et al. CDK4/6 inhibitors induce replication stress to cause long-term cell cycle withdrawal. EMBO J EMBO. 2022;41:e108599.
35. Yu X, Liu Y, Yin L, Peng Y, Peng Y, Gao Y, et al. Radiation-promoted CDC6 protein stability contributes to radioresistance by regulating senescence and epithelial to mesenchymal transition. Oncogene Springer Sci Bus Media LLC. 2019;38:549–63.

36. Ward IM, Chen J. Histone H2AX is phosphorylated in an ATR-dependent manner in response to replicational stress. J Biol Chem. 2001;276:47759–62.
37. Nickoloff JA, Jaiswal AS, Sharma N, Williamson EA, Tran MT, Arris D, et al. Cellular responses to widespread DNA replication stress. Int J Mol Sci MDPI AG. 2023;24:16903.
38. Luczak MW, Zhitkovich A. Monoubiquitinated gamma-H2AX: Abundant product and specific biomarker for non-apoptotic DNA double-strand breaks. Toxicol Appl Pharmacol. 2018;355:238–46.
39. O'neill E, Imaging DNA. Damage Repair In Vivo After (177)Lu-DOTATATE Therapy. J Nucl Med. 2020;61:743–50.
40. Vijayaraghavan S, Karakas C, Doostan I, Chen X, Bui T, Yi M, et al. CDK4/6 and autophagy inhibitors synergistically induce senescence in Rb positive cytoplasmic cyclin E negative cancers. Nat Commun. 2017;8:15916.
41. Hafner M, Mills CE, Subramanian K, Chen C, Chung M, Boswell SA, et al. Multiomics Profiling Establishes the Polypharmacology of FDA-Approved CDK4/6 Inhibitors and the Potential for Differential Clinical Activity. Cell Chem Biol. 2019;26:1067–e10808.
42. Hsu C-H, Altschuler SJ, Wu LF. Patterns of Early p21 Dynamics Determine Proliferation-Senescence Cell Fate after Chemotherapy. Cell. 2019;178:361–e37312.
43. Ivanov A, Pawlikowski J, Manoharan I, van Tuyn J, Nelson DM, Rai TS, et al. Lysosome-mediated processing of chromatin in senescence. J Cell Biol. 2013;202:129–43.
44. Hino H, Iriyama N, Kokuba H, Kazama H, Moriya S, Takano N, et al. Abemaciclib induces atypical cell death in cancer cells characterized by formation of cytoplasmic vacuoles derived from lysosomes. Cancer Sci. 2020;111:2132–45.
45. Gong C, Lin Q, Qin T, Zeng Y, Xu F, Yang Y, et al. Targeting autophagy plus high-dose CDK4/6 inhibitors in advanced HR+HER2- breast cancer: A phase 1b/2 trial. Med (N Y). Elsevier BV. 2025;6:100559.
46. Han X, Chen H, Gong H, Tang X, Huang N, Xu W, et al. Autolysosomal degradation of cytosolic chromatin fragments antagonizes oxidative stress-induced senescence. J Biol Chem Elsevier BV. 2020;295:4451–63.
47. Miller KN, Li B, Pierce-Hoffman HR, Patel S, Lei X, Rajesh A, et al. p53 enhances DNA repair and suppresses cytoplasmic chromatin fragments and inflammation in senescent cells. Nat Commun Nat Publishing Group. 2025;16:2229.
48. Dou Z, Xu C, Donahue G, Shimi T, Pan J-A, Zhu J, et al. Autophagy mediates degradation of nuclear lamina. Nature. 2015;527:105–9.
49. Kraft LJ, Manral P, Dowler J, Kenworthy AK. Nuclear LC3 associates with slowly diffusing complexes that survey the nucleolus. Traffic Wiley. 2016;17:369–99.
50. Abella N, Brun S, Calvo M, Tapia O, Weber JD, Berciano MT, et al. Nucleolar disruption ensures nuclear accumulation of p21 upon DNA damage. Traffic. 2010;11:743–55.

51. Shen A, Wu M, Liu L, Chen Y, Chen X, Zhuang M, et al. Targeting NUFIP1 suppresses growth and induces senescence of colorectal cancer cells. Front Oncol Front Media SA. 2021;11:681425.
52. Maheshwari M, Yadav N, Hasanain M, Pandey P, Sahai R, Choyal K, et al. Inhibition of p21 activates Akt kinase to trigger ROS-induced autophagy and impacts on tumor growth rate. Cell Death Dis. 2022;13:1045.
53. Jo M, Kim S, Park J, Chang Y-T, Gwon Y. Reduced dynamicity and increased high-order protein assemblies in dense fibrillar component of the nucleolus under cellular senescence. Redox Biol Elsevier BV. 2024;75:103279.
54. Sun J, Salem HH, Bird P. Nucleolar and cytoplasmic localization of annexin V. FEBS Lett. 1992;314:425–9.
55. Barr AR, McClelland SE. Cells on lockdown: long-term consequences of CDK4/6 inhibition. EMBO J Springer Sci Bus Media LLC. 2022;41:e110764.
56. International Agency for Research on Cancer, Carneiro F, Hruban RH, Theise ND. In: Bosman FT, editor. WHO classification of tumours of the digestive system: Vol. Volume 3, 4 ed. IARC; 2010.
57. Magi-Galluzzi C. Prostate cancer: diagnostic criteria and role of immunohistochemistry. Mod Pathol Elsevier BV. 2018;31:S12–21.
58. Rajesh A, Havas AP, Arnold R, Lande K, Lei X, Li KY et al. Inhibiting cyclin D1-CDK6 suppresses senescence-associated inflammatory gene expression and age-related functional decline. Nat Aging. Springer Science and Business Media LLC; 2026;1–20.
59. Agarwal N, Castellano D, Alonso-Gordoa T, Arranz Arija JA, Colomba E, Gravis G, et al. A signal-finding study of abemaciclib in heavily pretreated patients with metastatic castration-resistant prostate cancer: Results from CYCLONE 1. Clin Cancer Res Am Association Cancer Res (AACR). 2024;30:2377–83.
60. Smith MR, Piulats JM, Todenhöfer T, Lee J-L, Arranz Arija JA, Mazilu L, et al. CYCLONE 2: A phase 3 study of abemaciclib with abiraterone in patients with metastatic castration-resistant prostate cancer. J Clin Oncol Am Soc Clin Oncol (ASCO). 2024;42:5001–5001.
61. de Kouchkovsky I, Rao A, Carneiro BA, Zhang L, Lewis C, Phone A, et al. A phase Ib/II study of the CDK4/6 inhibitor ribociclib in combination with docetaxel plus prednisone in metastatic castration-resistant prostate cancer. Clin Cancer Res Am Association Cancer Res (AACR). 2022;28:1531–9.
62. Grande E, Teulé A, Alonso-Gordoa T, Jiménez-Fonseca P, Benavent M, Capdevila J, et al. The PALBONET trial: A phase II study of palbociclib in metastatic grade 1 and 2 pancreatic neuroendocrine tumors (GETNE-1407). Oncologist. Volume 25. Oxford University Press (OUP); 2020. pp. 745–e1265.
63. Scheinberg T, Kench JG, Ferguson P, Sutherland S, Stockler MR, Mahon KL, et al. LEEP: A randomised, window of opportunity, neoadjuvant trial examining the pharmacodynamic effects of ribociclib prior to radical prostatectomy for high-risk, localised prostate cancer. J Clin Oncol Am Soc Clin Oncol (ASCO). 2025;43:392–392.

64. Wang B, Piccolantonio A, Altulea A, Huang M, Joshi T, Pagliarin F et al. Disruption of CDK4/6-RARα-NF-κB axis attenuates senescence-associated inflammation and improves function during aging and following chemotherapy. Nat Aging Springer Sci Bus Media LLC; 2026;1–15.
65. Seshadri V, Chng C, Tyler J, Adikerta C, Baghaei K, Wang Y, et al. Single-cell fluorescence imaging reveals heterogeneity in senescence biomarkers and identifies rapamycin-responsive sub-populations. Aging Cell Wiley. 2025;24:e70209.
66. de Zanger RMS, Chan HS, Breeman WAP, de Blois E. Maintaining radiochemical purity of [177Lu]Lu-DOTA-PSMA-617 for PRRT by reducing radiolysis. J Radioanal Nucl Chem. 2019;321:285–91.

Figures



Drug	Target	Drug	Target
SB 202190	p38 MAPK	Temsirolimus	mTOR
Talazoparib	PARP	Belinostat	HDAC
Tipifarnib	FTT/GGT	Rapamycin	mTOR
Abemaciclib	CDK4/6	AZD2461	PARP
Cryptotanshinone	natural product	Deforolimus	mTOR
TG100-115	PI3K	Everolimus	mTOR
AZ1775	Wee1	AP24534	BCR-ABL
LY500307	ERb	NU7441	DNA-PK
Olaparib	PARP	17-DMAG	HSP-90
Veliparib	PARP	SU11274	cMET
Mocetinostat	HDAC	AZ0156	ATM
Ribociclib	CDK4/6	PHA-680632	aurora kinase
Palbociclib	CDK4/6	KU-0063794	mTOR

Figure 1

Drug combination screen with ^{177}Lu-DOTATATE (a) CA20948 cells were exposed to ^{177}Lu-DOTATATE (0.32 MBq/mL, TRT), or vehicle, for 2 h, or exposed to an equitoxic dose (2.5 Gy) of external beam radiation (EBRT), washed and incubated on in varying concentrations of one of a panel of drugs. 12 days later, cells are stained to assess clonogenic survival. (**b**) Combination index of drug with EBRT or TRT was compared using LD50 values. Combination with 17-DMAG and olaparib are shown (**c**) Combination of ^{177}Lu-DOTATATE with the CDK4/6 inhibitor abemaciclib showed evidence of degree of synergy (CI <1) but did not show synergy in combination with EBRT. (**d**) Other CDK4/6i showed evidence of synergy alongside several other DDRi and cytostatic inhibitors.

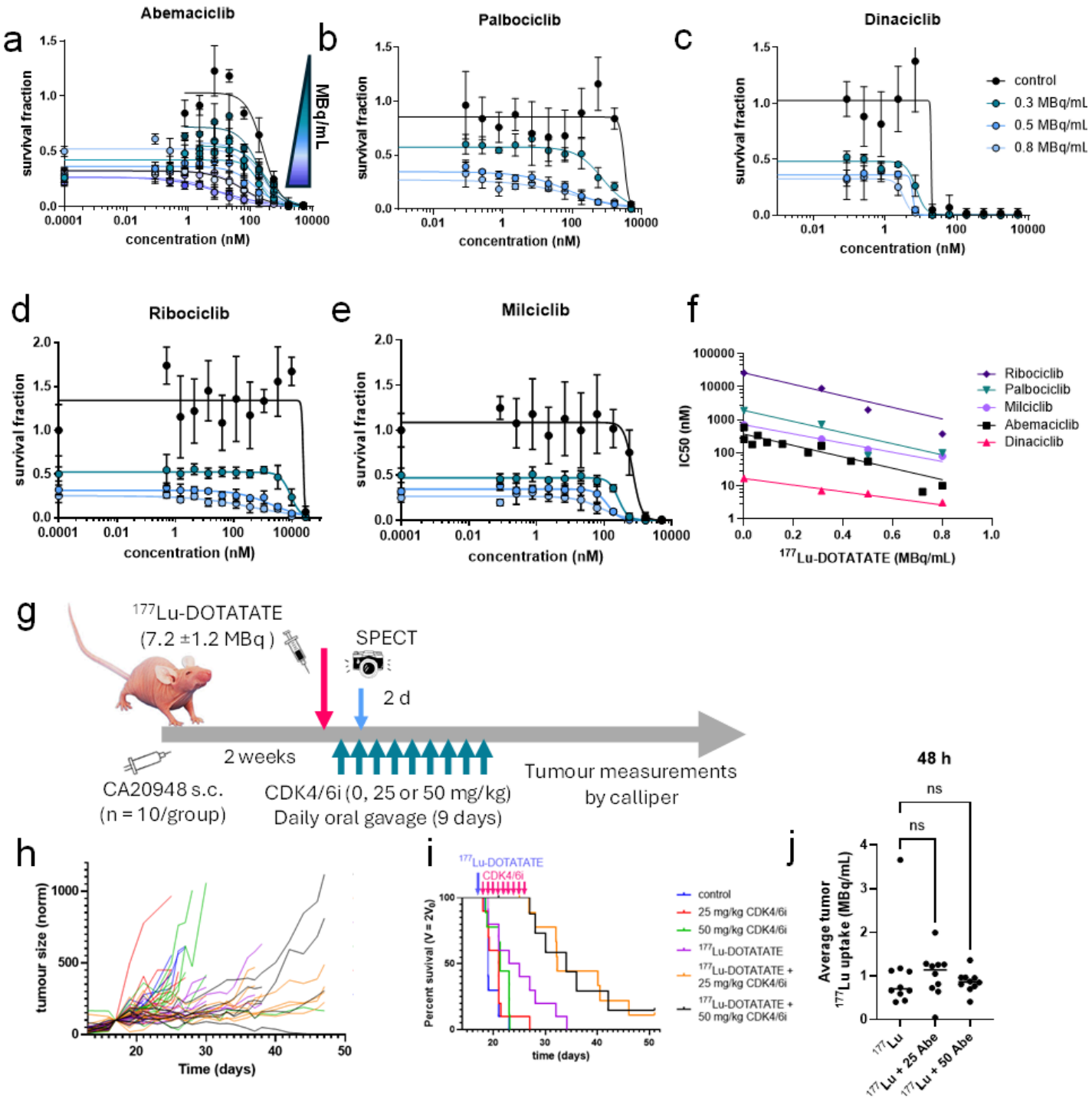


Figure 2

Combination hit validation with CDK inhibitors (a-e) A panel of structurally different CDK4/6 inhibitors are synergistic with ^{177}Lu-DOTATATE in CA20948 cells. **(f)** IC50 values of all CDK4/6 inhibitors are lower when combined with increasing concentrations of ^{177}Lu-DOTATATE indicative of a co-operative drug interaction. **(g)** Mice bearing subcutaneous CA20948 xenografts were administered a subtherapeutic activity of ^{177}Lu-DOTATATE (7.2 ± 1.2 MBq). Starting 24 h later, abemaciclib (25 or 50 mg/kg) or vehicle

control was administered by oral gavage daily for 9 days. **(h)** Tumour size was recorded by external callipers, and **(i)** survival (time to reach a doubling of tumour size relatively to the time of ^{177}Lu-DOTATATE administration) was significantly enhanced in the combination condition compared to monotherapies. **(j)** There was no significant difference in uptake of ^{177}Lu between treatment groups.

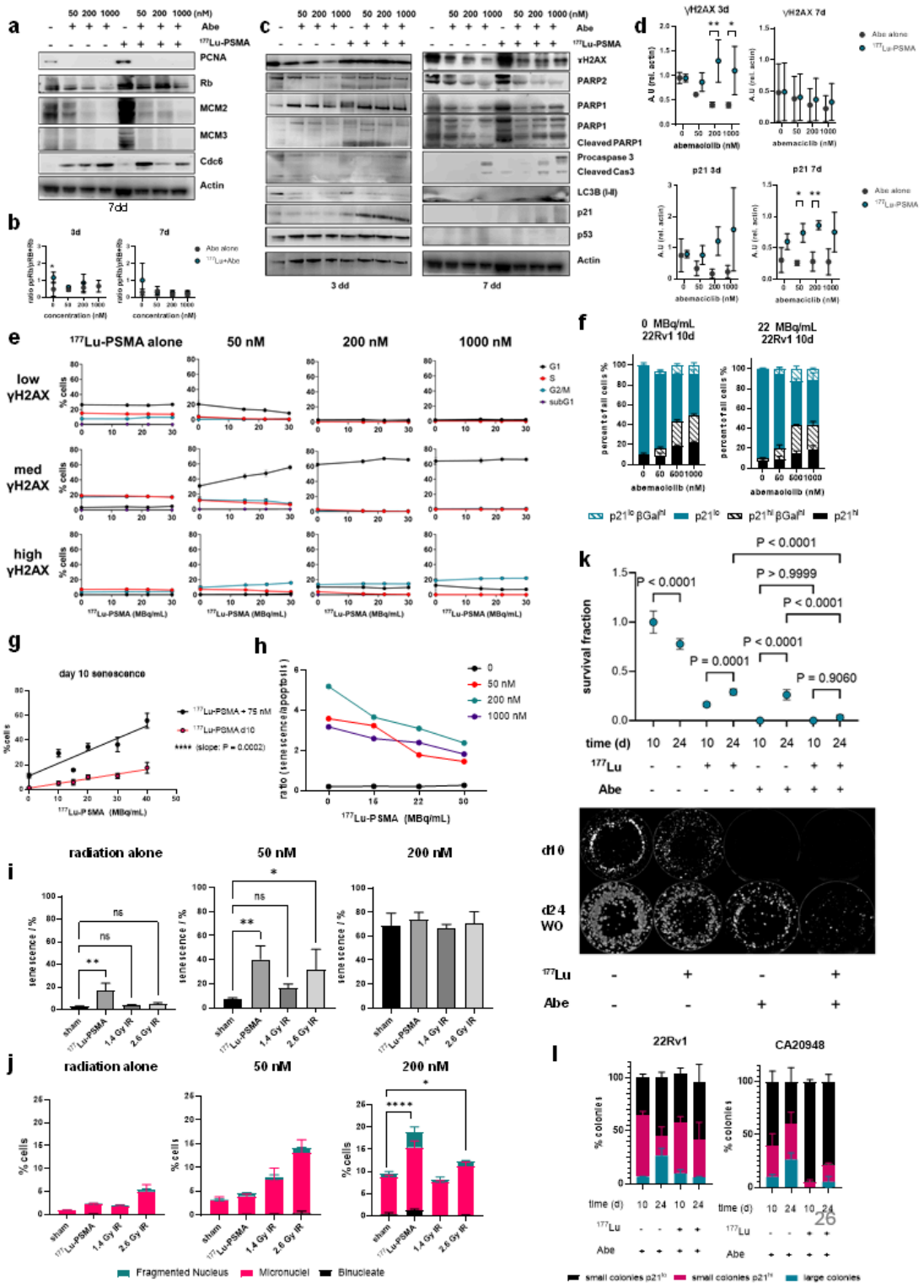


Figure 3

^{177}Lu TRT and CDK4/6i co-operate to increase replication stress, DNA damage, genotoxicity, and senescence (a-d) 22RV1 cells were treated with ^{177}Lu-PSMA, respectively, for a brief time, or vehicle, washed and incubated on in abemaciclib or vehicle control. **(a)** The concentrations of CDK4/6i active in combination with TRT from clonogenic studies caused a depletion of the replisome causing replication stress rather than cell cycle arrest as there was **(b)** no evidence of modulation of ppRb levels compared to control. **(c,d)** The combination of CDK4/6i and ^{177}Lu resulted in increased levels of DNA damage response marker γH2AX and accumulation of p21. **(e)** γH2AX levels after 10 days were elevated in response to CDK4/6i which increased with higher exposures to ^{177}Lu TRT. **(f)** CDK4/6i ^{177}Lu TRT combination greatly increases p21 associated senescence, **(g)** with a dose-dependent increase in senescence with ^{177}Lu TRT. **(h)** The addition of CDK4/6i resulted in increased induction of senescence (SA-β-Gal^{+}) relative to apoptosis/necrosis (Annexin V and/or PI +) compared to the static ratio of TRT alone. **(i)** TRT combination with CDK4/6i resulted in greater senescence induction at lower doses of CDK4/6i compared to EBRT, but there was no difference beyond 200 nM. **(j)** Genotoxicity was however greater with higher concentrations of CDK4/6i with TRT compared to EBRT. **(k)** CDK4/6i TRT combination resulted in permanent senescence induction in a longer-term wash-out clonogenic experiment where colonies were left to recover for another 14 days resulting in significant regrowth in 22Rv1 cells treated with monotherapies of CDK4/6i and ^{177}Lu-PSMA.

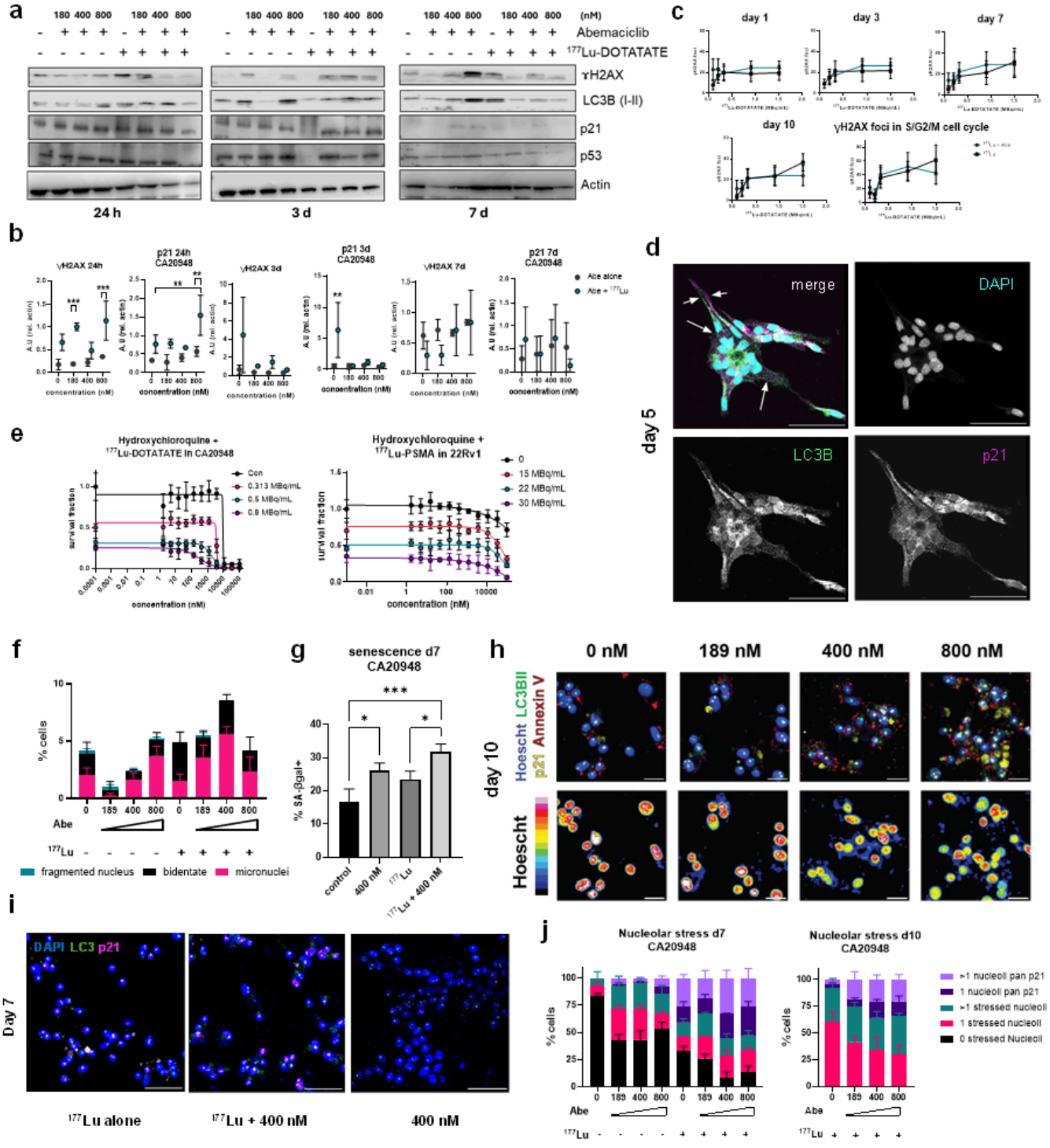


Figure 4

CDK4/6 inhibition can interfere with autophagy-dependent radioresistance towards ^{177}Lu TRT. (a,b) Despite an early increase in p21 and γH2AX protein levels at 24h in CA20948 there was a lack of sustained expression at later timepoints (3d and 7d). Fluctuating levels of LC3B indicated potential involvement of macroautophagy as a potential route to clear p21 and γH2AX protein levels. (**c**) The addition of abemaciclib did not significantly increase γH2AX foci in G1 cells over days 1-10, or S/G2/M

(day 7), but there was an apparent threshold limit of the number of γH2AX foci despite greater activity concentrations of ^{177}Lu-DOTATATE above 0.32 MBq/mL. (**d**) characteristic CDK4/6i vacuoles were present in cells treated with the ^{177}Lu+Abe combination at day 5 after the initial burst of p21, with elevated LC3B levels in cells with greater p21 expression indicative of a potential macroautophagic clearance mechanism to clear excess p21. (**e**) Hydroxychloroquine (HCQ) was synergistic by colony formation assay in combination with ^{177}Lu-DOTATATE in CA20948 cells, but was not in 22Rv1 cells with ^{177}Lu-PSMA. (**f**) The addition of abemaciclib did not result in a large increase in the same indicative metrics of genotoxicity (fragmented nuclei, bidendate or micronuclei) when combined with ^{177}Lu-DOTATATE (n=3, visually counted with fields containing at least 100 cells). (**g**) senescence (SA-β-Gal) was increased with the addition of abemaciclib (400 nM) at day 7 with and without ^{177}Lu-DOTATATE (1.5 MBq/mL). (**h**) The addition of abemaciclib to cells treated with ^{177}Lu-DOTATATE (1.5 MBq/mL) resulted in increased dsDNA staining outside the nucleus with increased expression of cytoplasmic p21 and Annexin V puncta, with nuclear focal uptake of LC3 and p21 within the nucleolus. (**I,j**) LC3 accumulation within the nucleolus was indicative of potential nucleolar stress, with many cells demonstrating decreased capacity to absorb further p21 with extra-nucleolus pan-nuclear expression of p21. These stressed nucleoli metrics were greater with the addition of ^{177}Lu-DOTATATE (1.5 MBq/mL) and was dose-dependent with the addition of abemaciclib, that was sustained from day 7 to day 10.

Supplementary Files

This is a list of supplementary files associated with this preprint. Click to download.

- SupplementalMethods.docx
- Combinationdrugscreen.xlsx
- sequencingresultsCRCA20948exome.xlsx
- Supplementaryfigures.docx
- Supplementarydatagelsandblots.docx
- SupplementaryFigures.docx